Probing the X-ray Spectra of Alpha Coronae Borealis

B. A. Korany [a,b].

[a] Department of Physics, Faculty of Applied Science, Umm Al-Qura University, Saudi Arabia.
[b] Department of Astronomy, National Research Institute of Astronomy and Geophysics (NRIAG), Helwan, Cairo, Egypt

A R T I C L E   I N F O

A B S T R A C T

In this context, I presented a detailed spectral and timing analysis of X-ray observations of the brightest eclipsing system Alpha Coronae Borealis taken by XMM-Newton. We got from the thermal plasma metal model the abundances of some elements (O, Mg, Si, and Fe) and an emission line at 1.3 Kev from the simple Gaussian line profile. From the light curves, there is a strong, active region at the lower left of the maps, near the limb of the G component, and increasing in some parts, which means a band diagonally, runs across the G star disk from lower left to upper right, close to the projected center.

1. Introduction

Alpha Coronae Borealis (α CrB) is one of the brightest eclipsing systems; so many studies were interested in this system in different energy bands. Stebbins [1] discussed it early in an optical band [2]. Tomkin [3] gives detailed optical information for this system as; it is a 17.4 day eclipsing binary, the spectral types of its components are A and G with different masses, the G- type component is a dwarf star in a 17.4 day orbital period, and the system orbital property is i=88.2, rp =0.07±0.007, rs = 0.021±0.001. Schmitt, in 2016, used the TIGRE 1.2 m telescope observation to get a new radial velocity curve, apsidal motion, and the alignment of the rotation and orbit axes. The apsidal motion rate $0.035 < \omega < 0.054$ degrees/year and the apsidal motion period (Paps) is in the range of 6600 yr < Paps < 10 600 yr, while the apsidal motion values results in a difference of 7.2 s $< \Delta Psp = Ps - Pp < 11.6$ s [4].

The First X-ray observation of this system was by ROSAT in 1993 [2]. Schmitt and Kurster [2,5] reconstructed a rough surface X-ray map, applying a maximum likelihood method. The resulting map revealed a patchy surface coverage of X-ray emitting material. The X-ray light curve of α CrB shows a total X-ray eclipse during the secondary optical minimum with the G star behind the A star. The totality of the eclipse demonstrates that the A-type component in α CrB is X-ray dark and that the x-ray flux arises exclusively from the later-type companion [2]. Güdel et al. [6] used X-ray data, observed by XMM-Newton, during a total X-ray eclipse of this binary system and studied the tomography of a stellar X-ray corona. They calculated the binary orbital elements (a, e, i, ω: 2.981 × 1012 cm, 0.370, 88.2o, 311.0o respectively) and the stellar radii are RA=3.04 RϴΘ and RG =0.09 RϴΘ.

We report in this paper the spectral and timing analysis of X-ray observations of the eclipsing system α CrB , taken by XMM-Newton observations. We organized the paper as follows: The X-Ray observations and data reduction are presented in section 2, section 3 is devoted to the spectral analysis, while the results are summarized and concluded in section 4.

2. X-Ray Observations and data reduction

We used XMM-Newton observations for α CrB from the XMM-Newton archive; the observing log is given in Table 1. All EPIC cameras were operated in the small-window mode with the thick filter inserted in order to suppress the strong optical flux from the primary A star [6]. We made use of the data from the two EPIC MOS [7] cameras and the EPIC PN camera [8]. The raw data were processed with the EPIC pipeline chains of the Science Analysis System (SAS) software version 9.0. Some bad time intervals, characterized by high background events (so-called soft-proton flares), were rejected by creating light-curves for the observations (PN, MOS1, and MOS2), which are best visible above 10 Kev. To optimize the signal-to-noise ratio in the light curve and to suppress large background contributions and contributions from warm pixels in the very soft range. Because of the poverty of the hard x-ray photons of this object, the only soft X-Ray band extracted exclusively is in the energy range 0.30-2.0 Kev for the PN and 0.14-2.5 Kev for the MOS1&MOS2 cameras. The spectrum of the star was extracted using circular extraction regions centered on the star, with radii of approximately 25" for both the MOS and PN cameras. In order to utilize the $\chi 2$ technique, the X-ray spectra were rebinned to contain at least 20 counts in each spectral bin using grppha command. All the spectra were subsequently analyzed using the Xspec software (v12).

For the timing analysis, we extracted the source and background light curve by using the evselect task of SAS software version 9.0. The light curves obtained were corrected to account for a number of effects, which an impact in the detection efficiency can have like; vignetting, bad pixels, PSF variation and quantum efficiency, as well as to account for time-dependent corrections within an exposure, like dead time and GTIs, by using the SAS task epiclccorr. Because in the short time periods of the x-ray binaries, the arrival time of a photon is shifted as it would have been detected at the barycenter of the solar system (the center of mass) instead of the position of the satellite. In this way, the data are comparable. We used the SAS barycen to correct these timestamps to the Earth's barycenter for each event. The Xronos program package was used to make a timing analysis (producing a binned light curve, calculating a power spectrum, searching for periodicities etc.).

Table 1. Observing log for α CrB with XMM-Newton

Instrument	Mode	Filter	Date @Exp. Start Time	Date @ Exp. End Time
MOS1	Small-window	THICK FILTER	2001-08-27 @04:42:44	2001-08-27 @15:42:18
MOS2	Small-window	THICK FILTER	2001-08-27 @04:42:44	2001-08-27 @15:42:18
PN	Small-window	THICK FILTER	2001-08-27 @04:58:46	2001-08-27 @15:43:09

---

[*] **Corresponding Author**

Department of Physics, Faculty of Applied Science, Umm Al-Qura University, Saudi Arabia.
E-mail address: **baewiss@uqu.edu.sa**

3. X-Ray Data Analyses

The first model used to fit the spectra was a single temperature variable-abundance thermal plasma model. In this model, an emission spectrum from hot diffused gas based on the model calculations of Mewe and Kaastra with Fe L calculations. The model includes line emissions from several elements. The He element in the model was fixed at cosmic, and the normalization was calculated from following equation:

$$\frac{10^{-14}}{4\,\pi[D_A(1+z)]^2}\int n_e n_H\, dv \tag{1}$$

where DA is the angular diameter distance to the source in cm, ne & nH are the densities in cm^{-3} of the electron and hydrogen respectively [8] (in Xspec software this model called vmekal). Figures 1 to 3 explains the fit for PN and MOS, while Figure 4 is the fitting of the three detectors (PN, MOS1, and MOS2 respectively). The elements of metal abundance included in the model are C, N, O, Ne, Na, Mg, Al, Si, S, Ar, Ca, Fe and Ni. We set O, Ne, Mg, Si, S, and Fe are free parameters in the fit. We got a best fit for this single model, χ^2/odf is 141.16/121. The output temperature is 0.46±0.02, while the output values of the abundance of the elements O, Mg, S, and Fe are 0.25±0.05, 0.44±0.12, 0.52±0.27 and 0.26±0.02 respectively. The X-ray luminosity evaluated from 0.3-10.0 Kev is 5.3×10^{28} erg s^{-1}, which agrees with the luminosity reported previously [2,6]. By adding the A photo-electric absorption due to the hydrogen column density, no significant change in the fitting was seen (the results are summarized in Table 2). The simple Gaussian line profile, which was calculated from the equation

$$A(E) = K\frac{1}{\sigma\sqrt{(2\times\pi^2)}}e^{\left(\frac{-(E-E_t)^2}{2\sigma^2}\right)} \tag{2}$$

(here Et is the line energy in Kev, σ is the line width in Kev and K is the total photons/cm^{-2}/s in the line), was applied, the fitting was improved (χ^2/ odf = 123.75/ 107) (the fitting of the thermal plasma model with simple gaussian line for PN data shown in Figure 5) and we got an emission line at 1.3 Kev (all the parameter in Table 2).

The produced binned light curve for the three detectors (PN, MOS1, and MOS2) explains that the data covers the complete second eclipse (Figures 6-9). The gross shape of the ingress and egress portions of the curve is symmetric; the total ingress and egress durations are 2.74 and 1.66 hrs, respectively. During ingress and egress, a sequence of fast drops/rises in flux and several flux plateaus are evident. We can note from the light-carve figures, a strong asymmetry in all light curves, and the individual steep flux decreases and increases. We can see from Figures 5 to 7 a strong active region at the lower left of the maps, near the limb of the G component, the lower right part which in increasing means a band diagonally runs across the G star disk from lower left to upper right, close to the projected center. The upper right part has the same features as the lower part, but weaker band displaced somewhat to the right, and to the bright source of the upper right secondary limb. The banded structure from lower left to upper right may partially be an artifact since the ingress light curve decays relatively smoothly below feature of the lower right part.
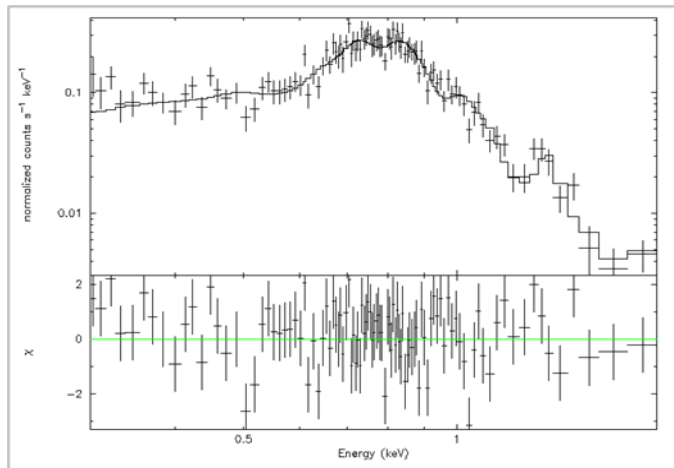

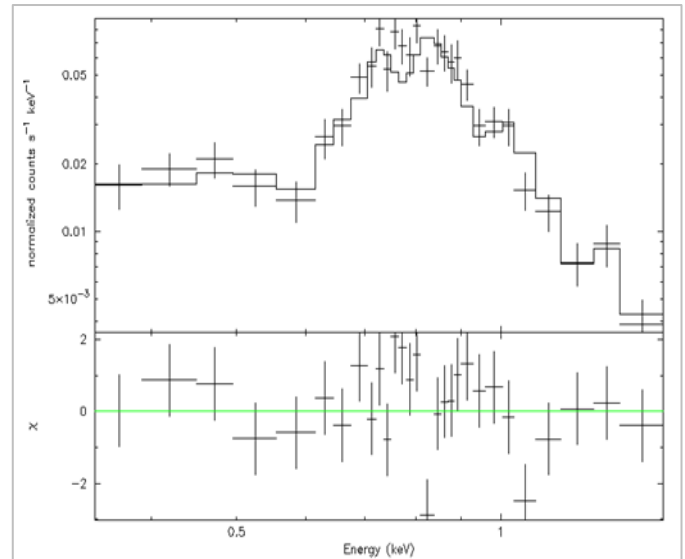**Figure 1**: The EPIC PN spectrum which fitted using single thermal plasma model, with χ^2 test.

Figure 2: The EPIC MOS1 spectrum which fitted using single thermal plasma model, with χ^2 test.
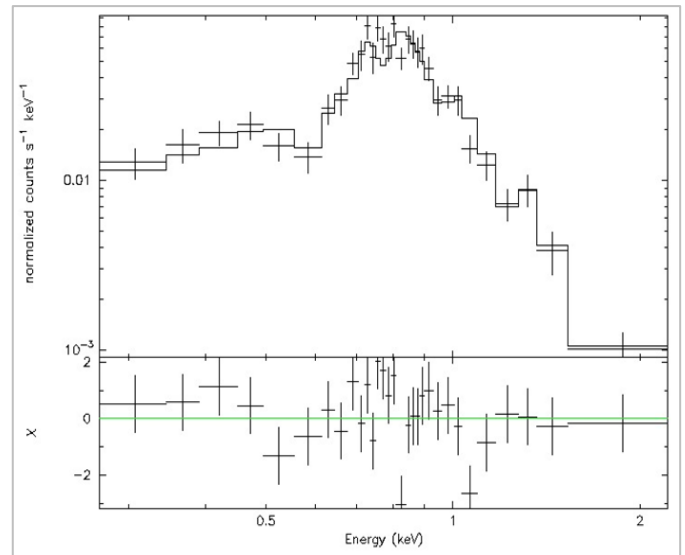

Figure 3: The EPIC MOS2 spectrum which fitted using single thermal plasma model, with χ^2 test.
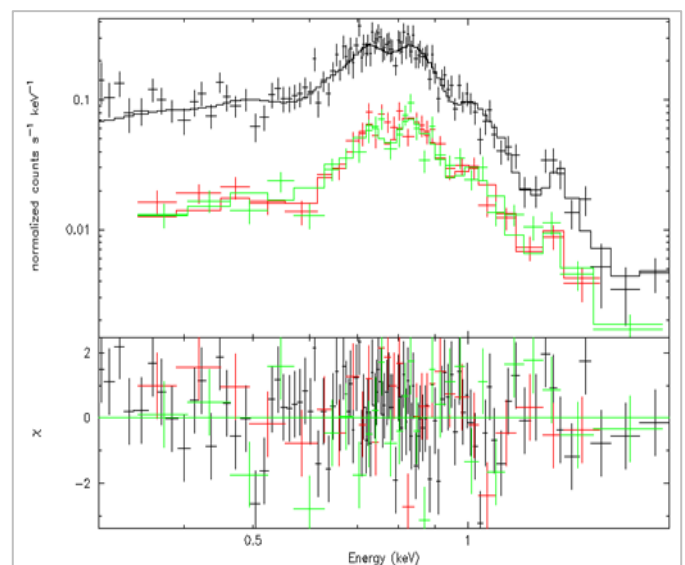

Figure 4: The EPIC PN, MOS1 and MOS2 spectra which fitted using single thermal plasma model, with χ^2 test.
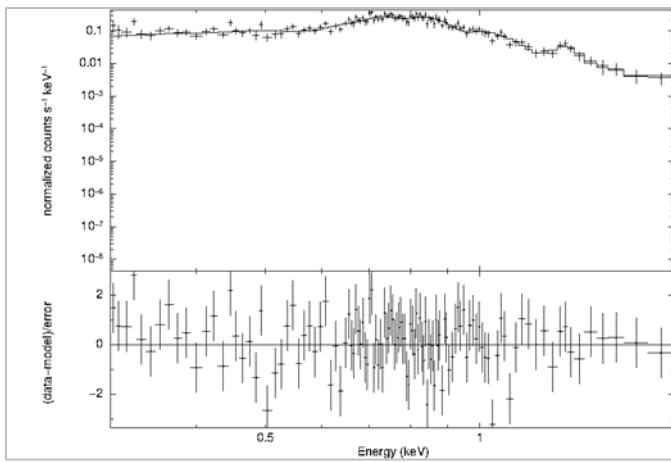
Figure 5: The EPIC PN spectrum which fitted using single thermal plasma Model and single gaussian line, with χ^2 test.

Table 2. Summarizing the parameters of the output fitting

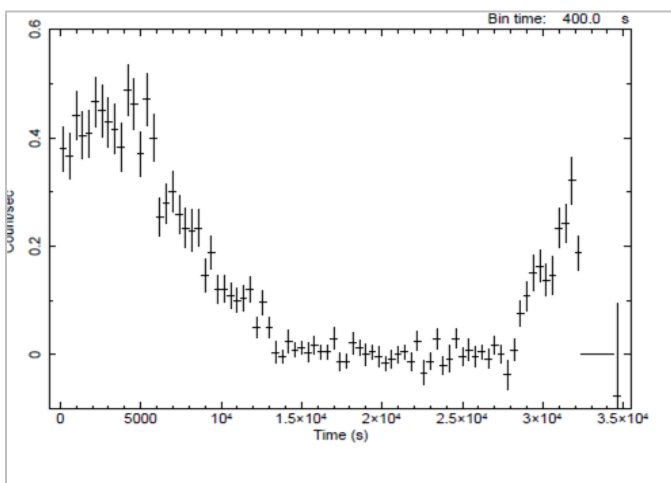| Parameter	Thermal plasma model	Thermal plasma model+ A photo-electric absorption	Thermal plasma model+ Gaussian line
Kt	0.46 ±0.02 Kev	0.46 ±0.02 Kev	0.47 ±0.02 Kev
O	0.25 ±0.05	0.27±0.06	0.33±0.06
Mg	0.44±0.12	0.47±0.13	0.54±0.16
Si	0.52±0.17	0.56±0.28	0.37±0.19
Fe	0.26±0.02	0.28±0.03	0.31±0.06
χ^2/odf	141.16/121	140.65/111	123.75/107
Normalization	2.5×10^{-4}	2.4×10^{-4}	2.6×10^{-5}

Figure 6: The X-ray light curve for PN data
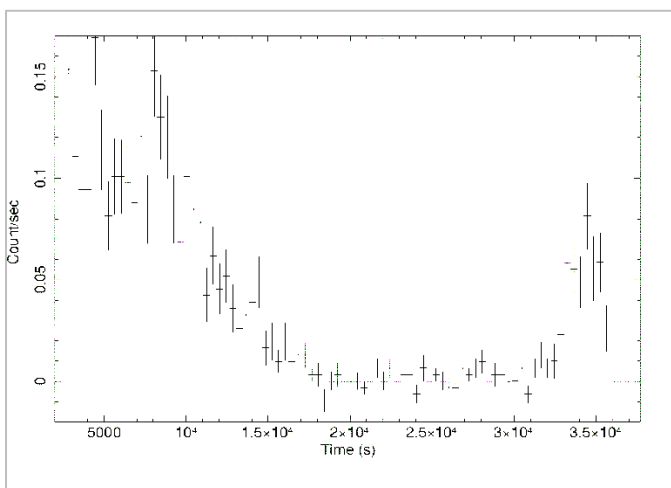

Figure 7: The X-ray light curve for MOS1 data
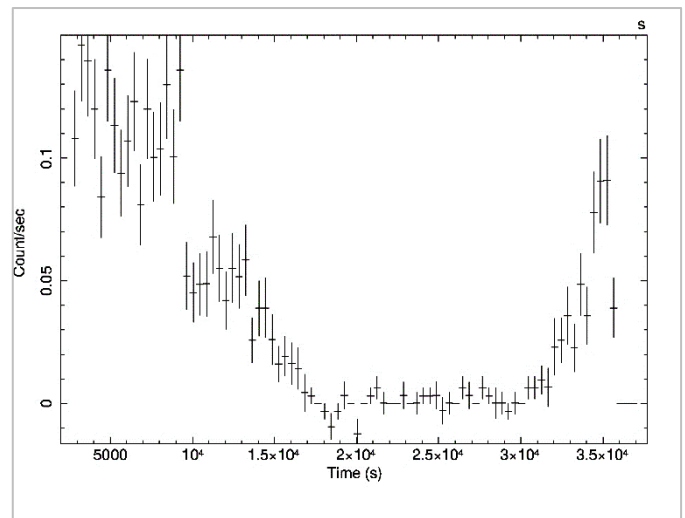

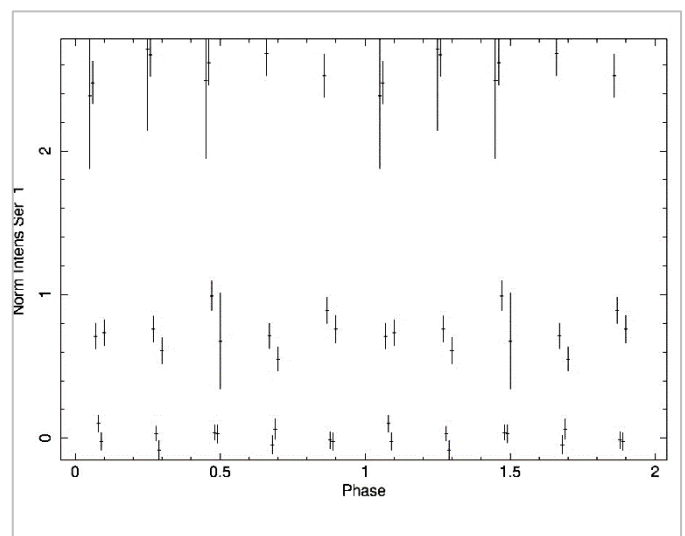**Figure 8**: The X-ray light curve for MOS2 data

Figure 9: Phase of the eclipsing binary

4. Discussion and conclusions

A detailed spectral and timing analysis (EPIC) has been performed for XMM-Newton observation of the alpha Coronae Borealis (α CrB) system. The soft X-Ray range (0.3-2.0 Kev) is described by three models. From these models, we got the best-fit temperature in the range 0.45 to 0.47 Kev, while the abundances of the elements O, Mg, Si and Fe that have the range 0.25 to 0.33, 0.44 to 0.54, 0.37 to 0.56 and 0.26 to 0.31 respectively, are low compared to solar photospheric values. By using Guessing model there is an emission line at 1.3 Kev. From the timing analysis there is a strong active region at the lower left of the maps, near the limb of the G component, and increasing in some parts means a band diagonally runs across the G star disk from lower left to upper right, close to the projected center. Some parts indicated that a weaker band displaced somewhat to the right, and to the bright source of the upper right secondary limb. The banded structure from lower left to upper right may partially be an artifact since the ingress light curve decays relatively smoothly below feature of the lower right part.

References

[1] Güdel, M., Arzner, K., Audard, M., and Mewe, R., Tomography of a stellar X-ray corona: alpha Coronae Borealis, 2003, A&A, 403, 155-171
[2] Liedahl, D.A., Osterheld, A.L., and Goldstein, W.H., New Calculations of Fe L-Shell X-Ray Spectra in High-Temperature Plasmas, 1995, ApJL, 438, 115-127
[3] Schmitt, J. H. M. M., & Kürster, M., A Spatially Resolved X-ray Image of a Star Like the Sun, 1993, Science, 262, 215-226

[4] Schmitt1, J. H. M. M., Schröder, K.-P., Rauw, G., Hempelmann, Mittag, A, M. , González-Pérez1 J. N., Czesla1, S., Wolter, U., and Jack, D., The α CrB binary system: A new radial velocity curve, apsidal motion, and the alignment of rotation and orbit axes, A&A, 2016, 586, 1-13

[5] Schmitt, J. H. M. M., & Kürster, M., APS Conference Series, The Eclipsing X-Ray Binary alpha CrB, 1994, 64, 137-150

[6] Strüder, L.; Briel, U.; Dennerl, K.; The European Photon Imaging Camera on XMM-Newton: The pn-CCD camera, 2001, A&A, 365, L18-L26

[7] Turner, M. J. L., Abbey, A., Arnaud, M., The European Photon Imaging Camera on XMM-Newton: The MOS cameras, 2001, A&A, 365, 27-35

[8] Tomkin, J. and Popper, D. M, Rediscussion of eclipsing binarties. XV. Alpha Coronae Borealis, a main-sequence system with components of types A and G. ,1968 , AJ   92, 1428-1437